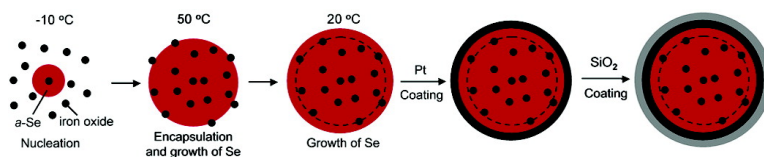


## Amorphous Se: A New Platform for Synthesizing Superparamagnetic Colloids with Controllable Surfaces

Unyong Jeong, Thurston Herricks, Edan Shahar, and Younan Xia

*J. Am. Chem. Soc.*, **2005**, 127 (4), 1098-1099 • DOI: 10.1021/ja043847u • Publication Date (Web): 06 January 2005

Downloaded from <http://pubs.acs.org> on March 24, 2009



### More About This Article

Additional resources and features associated with this article are available within the HTML version:

- Supporting Information
- Links to the 11 articles that cite this article, as of the time of this article download
- Access to high resolution figures
- Links to articles and content related to this article
- Copyright permission to reproduce figures and/or text from this article

[View the Full Text HTML](#)

## Amorphous Se: A New Platform for Synthesizing Superparamagnetic Colloids with Controllable Surfaces

Unyong Jeong, Thurston Herricks, Edan Shahar, and Younan Xia\*

Department of Chemistry, University of Washington, Seattle, Washington 98195-1700

Received October 8, 2004; E-mail: xia@chem.washington.edu

Colloidal particles have found widespread use in many areas such as chemical engineering, pharmaceuticals, photonics, and biotechnology. Superparamagnetic colloids, in particular, have been actively explored in the form of nano- and microparticles for applications in biomedical separation and diagnostics,<sup>1</sup> magnetic information storage,<sup>2</sup> and ferrofluidic technology.<sup>3</sup> For most of these applications, it is important to have good control over the surface functionalities of these colloidal particles. To this end, a number of procedures have been demonstrated to encapsulate superparamagnetic nanoparticles (e.g., iron oxides) in colloidal particles made of organic polymers<sup>4</sup> or silica.<sup>5</sup> Although these materials allow further surface modification via the use of self-assembled monolayers (SAMs),<sup>6</sup> it has been far more difficult to control the quality of resultant SAMs when compared to the system based on alkanethiols and coinage metals.<sup>7</sup> For colloidal particles made of polymers or silica, it is possible to coat their surfaces with coinage metals,<sup>8</sup> albeit the coating layers are usually characterized with problems such as low coverage, poor adhesion, surface roughing, and degradation in size uniformity. Here we report a new system based on amorphous selenium (*a*-Se) which enables the synthesis of monodispersed spherical colloids that exhibit both superparamagnetism and controllable surfaces.

Figure 1 outlines the synthetic approach. Uniform colloids of *a*-Se were produced in ethylene glycol (EG) via the reduction of selenious acid with excess hydrazine.<sup>9</sup> The key to the success of this synthesis was the use of temperature regulation to control the encapsulation of iron oxide nanoparticles and the growth of *a*-Se colloids. In the first step, iron oxide nanoparticles, hydrazine, and selenious acid were successively added to EG held at  $-10\text{ }^{\circ}\text{C}$ . The slow reduction rate at this temperature greatly promoted the role of iron oxide particles as exotic nuclei. The product involved in this stage was mainly individual iron oxide nanoparticles coated with thin shells of *a*-Se. After 20 min, the temperature was raised to  $50\text{ }^{\circ}\text{C}$ . Since the glass transition temperature of Se is  $32\text{ }^{\circ}\text{C}$ ,<sup>10</sup> the surfaces of *a*-Se colloids were softened and therefore became "sticky" to iron oxide nanoparticles. In addition, the enhanced reduction rate facilitated continuous encapsulation of iron oxide nanoparticles into the *a*-Se colloids. After 10 min, the temperature was reduced to  $20\text{ }^{\circ}\text{C}$  to harden the surfaces of *a*-Se colloids and to slow their growth. In this case, it became difficult for the *a*-Se colloids to capture additional iron oxide nanoparticles from the solution phase. After residual hydrazine was removed from the solution and poly(vinyl pyrrolidone) (PVP) was added,  $\text{PtCl}_2$  was introduced at  $60\text{ }^{\circ}\text{C}$  and reduced to form conformal coatings on the *a*-Se colloids.<sup>11</sup> If necessary, the Pt-coated colloids could be further coated with amorphous  $\text{SiO}_2$  using the Stöber process.<sup>12</sup> In contrast,  $\text{SiO}_2$  could not be directly formed on *a*-Se colloids without the Pt layer. Both Pt- and  $\text{SiO}_2$ -coated *a*-Se colloids were uniform in size and exhibited smooth surfaces. More importantly, the Pt surface can be readily derivatized with SAMs of alkylisocyanide<sup>13</sup> or alkanethiols<sup>14</sup> and  $\text{SiO}_2$  can be modified with siloxane-based

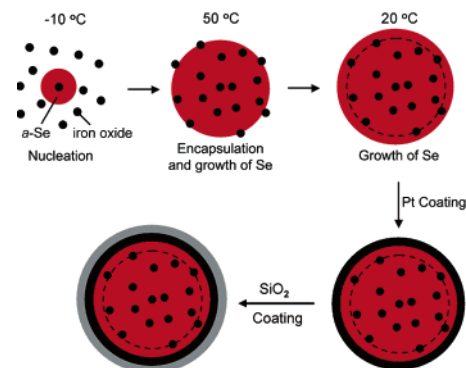


**Figure 1.** Outline of the experimental procedure. At  $-10\text{ }^{\circ}\text{C}$ , iron oxide nanoparticles serve as the nuclei for the growth of *a*-Se colloids. At  $50\text{ }^{\circ}\text{C}$  (above the  $T_g$  of Se), we could incorporate iron oxide particles into the growing *a*-Se colloids. At  $20\text{ }^{\circ}\text{C}$  (below the  $T_g$  of Se), *a*-Se grew without encapsulation of iron oxide particles. The dashed circle indicates that the surface ended at  $50\text{ }^{\circ}\text{C}$ . The surfaces of these colloids were further coated with Pt and  $\text{SiO}_2$  shells to prepare them for the formation of alkanethiolate and siloxane monolayers, respectively.

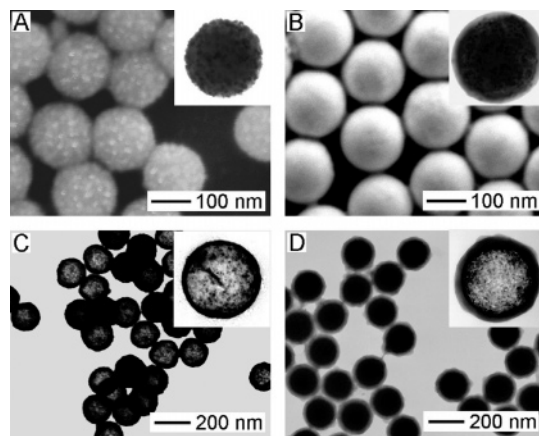


**Figure 2.** SEM and TEM images of colloids corresponding to each step shown in Figure 1. (A) SEM and TEM (inset) of the *a*-Se colloids prepared by quenching the solution from  $50$  to  $-10\text{ }^{\circ}\text{C}$ . (B) SEM and TEM (inset) of the *a*-Se colloids after completing the reaction at  $20\text{ }^{\circ}\text{C}$ . (C) TEM of the *a*-Se colloids after Pt coating. The inset shows a TEM of the colloid after its Se core had been removed with hydrazine. (D) TEM of the *a*-Se colloids whose surfaces had been coated with Pt and  $\text{SiO}_2$  shells. The inset shows a TEM image after removal of Se core.

SAMs.<sup>6</sup> Although thiolate SAMs on Pt provide a better control over the quality, siloxane SAMs on  $\text{SiO}_2$  offer higher thermal stability.<sup>6</sup>

Figure 2 gives SEM and TEM images corresponding to each step shown in Figure 1. Figure 2A illustrates the encapsulation of iron oxide nanoparticles at  $50\text{ }^{\circ}\text{C}$ . The sample was prepared by quenching the solution from  $50$  to  $-10\text{ }^{\circ}\text{C}$ . The SEM image indicates that many iron oxide nanoparticles were immobilized on each *a*-Se colloid to make the surface appear relatively rough. The

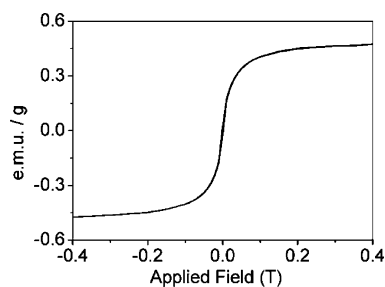


**Figure 3.** M–H curve of the Pt shells (see the inset of Figure 2C for a TEM image) at 300 K. Superparamagnetism was observed for all the colloids corresponding to each step of the synthesis illustrated in Figure 1.

TEM image in the inset implies that most of the iron oxide particles (dark spots) were embedded in the surface layer. Figure 2B shows an SEM image of *a*-Se colloids that were obtained after completing the reaction at 20 °C. The colloids displayed a very smooth surface, and the TEM image (inset) establishes that the surface layer was essentially free of iron oxide nanoparticles, suggesting that no encapsulation occurred at 20 °C. Figure 2C shows TEM image of the colloids after Pt coating, confirming the formation of Pt shells (~11 nm thick) with smooth surfaces and complete coverage. We also removed the *a*-Se cores with hydrazine since applications in biology and medical diagnosis require the magnetic colloids to be nontoxic and stable against sedimentation in the absence of an applied magnetic field. As shown in Figure S1 of the Supporting Information, the shape and crystal structure of the iron oxide nanoparticles were not affected by hydrazine. As shown in the inset of Figure 2C and the SEM image in Figure S2, the hollow Pt shells had enough structural rigidity to maintain their spherical shape. Figure 2D shows a TEM image of *a*-Se colloids whose interiors are embedded with iron oxide nanoparticles and surfaces are coated with Pt and then SiO<sub>2</sub> shells (~27 nm thick). The inset shows a TEM image of the double-shelled colloid after the *a*-Se core had been removed by hydrazine. It is expected that the mechanical strength and chemical stability of these hollow particles can be substantially enhanced through the formation of silica coating. It is worth pointing out that all the spherical colloids (with or without *a*-Se cores) shown in Figure 2, parts C and D, were superparamagnetic. Figure 3 shows a typical magnetization curve measured for hollow Pt shells whose interiors were loaded with iron oxide nanoparticles (see Figure 2C). The anionic surfactants on the surface of iron oxide nanoparticles were capable of preventing them from aggregation within the hollow Pt spheres.

The magnetic colloids shown in Figure 2, parts C and D, could be immediately used for bioconjugation. For example, the Pt-coated colloids could be derivatized with alkanethiols terminated with carboxylic group<sup>14</sup> and then used for protein immobilization.<sup>15</sup> Figure 4 shows a fluorescence microscopy image of the Pt-coated colloids after their surfaces had been modified with thiols and fluorescent IgG. A drop of the aqueous suspension was placed on a glass slide to let the solvent evaporate. The homogeneous green fluorescence establishes the validity of thiolate surface chemistry and its application to the immobilization of biomolecules. The colloids with IgG immobilized at their surfaces could also be aligned under magnetic field (see the inset in Figure 4). This demonstration suggests the ability to manipulate the biofunctionalized colloidal particles using an external magnetic field.

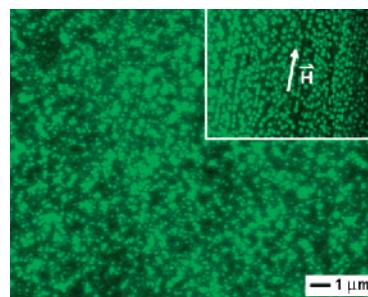


**Figure 4.** Fluorescence microscopy image of Pt-coated colloids whose surfaces had been derivatized with IgG containing fluorescence tag FITC. The colloids are randomly distributed on a glass slide when no magnetic field was applied. The inset shows magnetic alignment of these IgG-functionalized colloids. The sample was prepared by slowly evaporating a drop of the suspension under a magnetic field.

**Acknowledgment.** This work was supported in part by a DARPA-DURINT subcontract from Harvard University and a fellowship from the David and Lucile Packard Foundation. Y.X. is an Alfred P. Sloan Research Fellow and a Camille Dreyfus Teacher Scholar. U.J. has also been partially supported by the Postdoctoral Fellowship Program of the Korean Science and Engineering Foundation (KOSEF).

**Supporting Information Available:** Experimental procedures and materials, TEM images of iron oxide nanoparticles after hydrazine treatment, and SEM image and EDX spectrum of the Pt-coated colloids after removal of *a*-Se cores. This material is available free of charge via the Internet at <http://pubs.acs.org>.

## References

- (1) A special issue in *J. Phys. D: Appl. Phys.* **2003**, *36*, R167–R206.
- (2) (a) Murray, C. B.; Sun, S.; Doyle, H.; Betley, T. *Mater. Res. Soc. Bull.* **2001**, *26*, 985. (b) Hyeon, T. *Chem. Commun.* **2003**, 927.
- (3) Rosensweig, R. *Ferrohydrodynamics*; Cambridge University Press: Cambridge, 1985.
- (4) See, for example: (a) Dresco, P. A.; Zaitsev, V. S.; Gambino, R. J.; Chu, B. *Langmuir* **1999**, *15*, 1945. (b) Shihoh, H.; Manabe, Y.; Kawahashi, N. *J. Mater. Chem.* **2000**, *10*, 333. (c) Wormuth, K. *J. Colloid Interface Sci.* **2001**, *241*, 366. (d) Wang, Y.; Teng, X.; Wang, J.-S.; Yang, H. *Nano Lett.* **2003**, *3*, 789. (e) Xu, X.; Majetich, S. A.; Asher, S. A. *J. Am. Chem. Soc.* **2002**, *124*, 13864.
- (5) See, for example: (a) Tartaj, P.; González-Carreno, T.; Serna, C. J. *Adv. Mater.* **2001**, *13*, 1620. (b) Tartaj, P.; Serna, C. J. *Chem. Mater.* **2002**, *14*, 4396. (c) Lu, Y.; Yin, Y.; Mayers, B. T.; Xia, Y. *Nano Lett.* **2002**, *2*, 183. (d) Zeng, H.; Li, J.; Wang, Z. L.; Liu, J. P.; Sun, S. *Nano Lett.* **2004**, *4*, 187.
- (6) Ulman, A. *Introduction to Ultrathin Organic Films: From Langmuir-Blodgett to Self-Assembly*; Academic Press: Boston, 1991.
- (7) For a review, see: Whitesides, G. M.; Laibinis, P. E. *Langmuir* **1990**, *6*, 87.
- (8) (a) Westcott, S. L.; Oldenburg, S. J.; Lee, T. R.; Halas, N. J. *Langmuir* **1998**, *14*, 5396. (b) Dokoutchaev, A.; James, J. T.; Koene, S. C.; Pathak, S.; Prakash, G. K. S.; Thompson, M. E. *Chem. Mater.* **1999**, *11*, 2389. (c) Chen, C. W.; Serizawa, T.; Akashi, M. *Chem. Mater.* **1999**, *11*, 1381.
- (9) Jeong, U.; Xia, Y. *Adv. Mater.*, in press.
- (10) Zingaro, R. A.; Cooper, W. C. *Selenium*; Van Nostrand Reinhold: New York 1974; Chapter 1.
- (11) Mayers, B.; Jiang, X.; Sunderland, D.; Cattle, B.; Xia, Y. *J. Am. Chem. Soc.* **2003**, *125*, 13364.
- (12) Stöber, W.; Fink, A.; Bohn, E. *J. Colloid Interface Sci.* **1968**, *26*, 62.
- (13) See, for example: (a) Hickman, J. J.; Laibinis, P. E.; Auerbach, D. I.; Zou, C.; Gardner, T. J.; Whitesides, G. M.; Wrighton, M. S. *Langmuir* **1992**, *8*, 357. (b) Martin, B. R.; Dermody, D. J.; Reiss, B. D.; Fang, M.; Lyon, L. A.; Natan, M. J.; Mallouk, T. E. *Adv. Mater.* **1999**, *11*, 1021.
- (14) Geissler, M.; Chen, J.; Xia, Y. *Langmuir* **2004**, *20*, 6993.
- (15) See, for example: Frey, B. L.; Corn, R. M. *Anal. Chem.* **1996**, *68*, 3187.

JA043847U